High-Performance InP/$In_{0.53}Ga_{0.47}$As/InP Double HBTs on GaAs Substrates

Y. M. Kim, M. Dahlstrŏm, S. Lee, M. J. W. Rodwell, and A. C. Gossard

***Abstract*—InP/$In_{0.53}Ga_{0.47}$As/InP double heterojunction bipolar transistors (HBTs) were grown on GaAs substrates. A 140 GHz power-gain cutoff frequency $f_{\max}$ and a 207 GHz current-gain cutoff frequency f_τ were obtained, presently the highest reported values for metamorphic HBTs. The breakdown voltage BV_{CEO} was 5.5 V, while the dc current gain β was 76. High-thermal-conductivity InP metamorphic buffer layers were employed in order to minimize the device-thermal resistance.**

***Index Terms*—Heterojunction bipolar transistor, indium phosphide, metamorphic growth, molecular beam epitaxy.**

I. Introduction

DOUBLE heterojunction bipolar transistors [1]–[3] (DHBTs) have applications in high-frequency communications and radar. HBTs using InP based materials (InGaAs or GaAsSb epitaxial base layers and InGaAs or InP epitaxial collector layers) currently exhibit significantly higher current-gain and power-gain cutoff frequencies than GaAs-based HBTs. However, InP substrates are expensive and fragile and are readily broken during processing. This has motivated the investigation of metamorphic growth of InP-based DHBTs on GaAs substrates [4], [5]. To date, reported metamorphic HBTs (M-HBTs) have not yet demonstrated bandwidth comparable to that of lattice-matched InP HBTs. Further, thermal performance has not yet been addressed.

Wideband DHBTs operate at high power densities. Recently reported static frequency dividers operating at 75-GHz clock frequency [6] employ InP HBTs operating at 180 kA/cm^2 current density and $V_{CE} \sim 1.1$ V, corresponding to a power density per unit emitter junction area A_E of $P/A_E \sim 200$ kW/cm^2. Current density, hence power density, must further increase as logic speed is increased [6]. W-band DHBT power amplifiers also operate at high junction power densities. As shown in the seminal work by Liu and Chau [7], [8], because of the concentrated heat flux immediately below the HBT collector, DHBT thermal resistance is critically dependent upon the thermal resistance of layers lying immediately below the DHBT collector, and thick layers of low-thermal-conductivity ($\kappa = 5$ W/k-m) InGaAs must be avoided in the subcollector. M-DHBTs face a similar difficulty, because (as measured in our laboratory) InAlAs and AlGaAsSb metamorphic buffer layers also have very low thermal conductivity (10.5 W/K-m, and 8.4 W/K-m respectively). These layers are typically 1.5 μm thick and lie immediately below the DHBT subcollector.

TABLE I
LAYER STRUCTURE OF THE MBE-GROWN InP/$In_{0.53}Ga_{0.47}$As/InP METAMORPHIC DHBT. ALL GRADED LAYERS ARE $In_{0.53}Ga_{0.47}$As/$In_{0.52}Al_{0.48}$As DIGITAL ALLOY GRADES, EXCEPT THE BASE, WHICH IS AN In_xGa_{1-x}As LINEAR COMPOSITIONAL GRADE. THE BASE–COLLECTOR GRADE HAS A 15 Å PERIOD

Layer	Material	Doping	Thickness (Å)
Emitter cap	$In_{0.53}Ga_{0.47}$As	2×10^{19} cm^{-3}: Si	300
Grade	$In_{0.53}Ga_{0.47}$As to $In_{0.53}Ga_{0.26}Al_{0.21}$As	2×10^{19} cm^{-3}: Si	200
N$^+$ emitter	InP	2×10^{19} cm^{-3}: Si	700
N$^-$ emitter	InP	8×10^{17} cm^{-3}: Si	500
Emitter-base grade	$In_{0.53}Ga_{0.26}Al_{0.21}$As to $In_{0.455}Ga_{0.545}$As	4×10^{17} cm^{-3}: Si 8×10^{17} cm^{-3}: Be	233 47
Graded base	$In_{0.455}Ga_{0.545}$ As to $In_{0.53}Ga_{0.47}$As	4×10^{19} cm^{-3}: Be	400
Setback	$In_{0.53}Ga_{0.47}$As	2×10^{16} cm^{-3}: Si	100
Base-collector grade	$In_{0.53}Ga_{0.47}$As to $In_{0.53}Ga_{0.26}Al_{0.21}$As	2×10^{16} cm^{-3}: Si	240
Pulse doping	InP	5.6×10^{18} cm^{-3}: Si	30
Collector	InP	2×10^{16} cm^{-3}: Si	1,630
Subcollector	$In_{0.53}Ga_{0.47}$As	1×10^{19} cm^{-3}: Si	250
Subcollector	InP	2×10^{19} cm^{-3}: Si	750
Buffer	InP	undoped	15,000
GaAs (100) semi-insulating substrate			

Here we report InP-based DHBTs grown on GaAs using InP as the metamorphic buffer layer. This layer has a measured 16.1 W/K-m thermal conductivity. The current-gain and power-gain cutoff frequencies are $f_\tau = 207$ GHz and $f_{\max} = 140$ GHz, both records for M-DHBTs. An M-DHBT with 0.4 μm $\times$ 7.5 μm emitter area has a measured 2.8 K/mW thermal resistance, and exhibits a small measured 35 K junction-ambient temperature rise even when biased at $J_e = 190$ kA/cm^2 and $V_{ce} = 2$ V ($P/A_E = 380$ kW/cm^2). At $V_{CE} = 1.5$ V, f_τ and $f_{\max}$ collapse due to the Kirk effect (collector field screening) occurs at a high $J_e = 450$ kA/cm^2 current density.

II. Growth

InP/$In_{0.53}Ga_{0.47}$As/InP DHBTs were grown on a GaAs substrate using a Varian Gen II molecular beam epitaxy (MBE) system. Growth was initiated with a 1000 Å undoped GaAs buffer layer, followed by growth at 470 °C of a 1.5 μm undoped InP metamorphic buffer layer. The remaining HBT layers were then grown. Key features of the layer structure (Table I) include an InP emitter, a 400 Å InGaAs base with 52 meV band-gap

Manuscript received January 25, 2002. This work was supported by the Office of Naval Research under Grant N00014-01-1-0065. The review of this letter was arranged by Editor D. Ritter.

The authors are with the Department of Electrical and Computer Engineering, University of California, Santa Barbara, CA 93106 USA (e-mail: kymdow@ece.ucsb.edu).

Publisher Item Identifier S 0741-3106(02)04536-6.

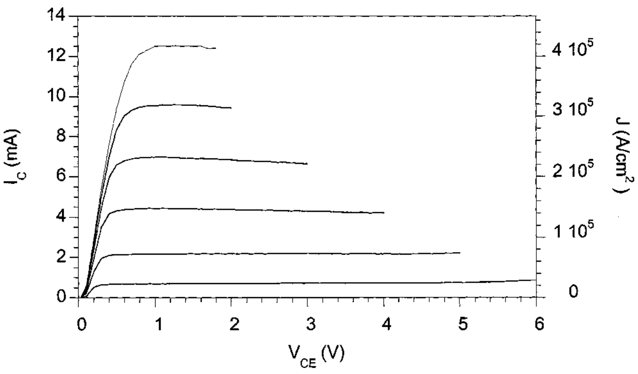

Fig. 1. Common emitter dc characteristics of 0.4 μm × 7.5 μm emitter device. The base-current steps are 40 μA.

grading for base transit time reduction, a 240 Å InGaAs/InAlAs base–collector heterojunction grade, and a 1660 Å InP collector. The heterojunction between the $In_{0.53}Ga_{0.47}As$ base and the InP collector is a 240 Å $In_{0.53}Ga_{0.47}As/In_{0.52}Al_{0.48}As$ chirped superlattice whose composition adjacent to the collector is $In_{0.53}Ga_{0.26}Al_{0.21}As$, chosen so as to eliminate discontinuities in the conduction-band energy at the interface. A similar superlattice grade is employed in the emitter–base junction. To reduce sensitivity to diffusion of the Be base dopant, a 100 Å undoped $In_{0.53}Ga_{0.47}As$ setback layer was introduced between the base and the base–collector grade. The total collector–base depletion region thickness is therefore 2000 Å. The metamorphically grown HBT layers are relatively rough (9.5 nm RMS, as determined by atomic force microscopy).

III. Fabrication

HBTs were fabricated in a triple-mesa process using optical projection lithography and selective wet chemical etching. Use of narrow emitter–base and collector–base junctions reduces both the base resistance and the collector–base capacitance [9]. While the emitter contact metal is 0.7 μm × 8 μm, lateral undercutting during the HCl-based etch of the InP emitter forms an emitter–base junction whose dimensions are approximately 0.4 μm × 7.5 μm. Collector–base capacitance is reduced by employing narrow base Ohmic contacts of 0.25 μm width on either side of the emitter stripe, producing a small 1.2 μm × 11 μm base–collector junction area. Polyimide is used both for passivation and for mesa planarization prior to interconnect deposition.

IV. Results

Fig. 1 shows the common emitter characteristics, measured from 0–400 kA/cm^2 current density. The measured dc current gain is approximately 76, the common-emitter open-circuit breakdown voltage at low current densities BV_{CEO} is greater than 6 V, while $V_{CE,SAT} < 0.8$ V at 400 kA/cm^2 current density. The measured sheet resistance of the metamorphic InP buffer layer is approximately 150 MΩ per square. The base sheet resistance is 1020 Ω per square. This sheet resistance was measured after the emitter mesa etch, which removes approximately the upper 100 Å of the base layer. The corresponding hole mobility is 51 cm^2 cm/V-s, 10% lower than we observed for similar lattice-matched DHBT growths.

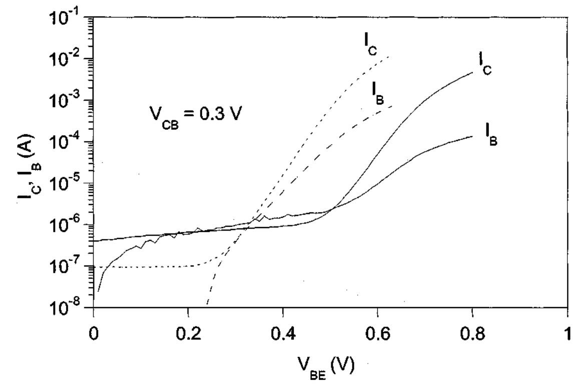

Fig. 2. Metamorphic HBT Gummel characteristics of (solid lines) an HBT with a 0.4 μm × 7.5 μm emitter–base junction and a 1.2 μm × 11 μm base–collector junction, and an HBT (dotted lines) with a 60 μm × 60 μm emitter–base junction and a 100 μm × 130 μm base–collector junction.

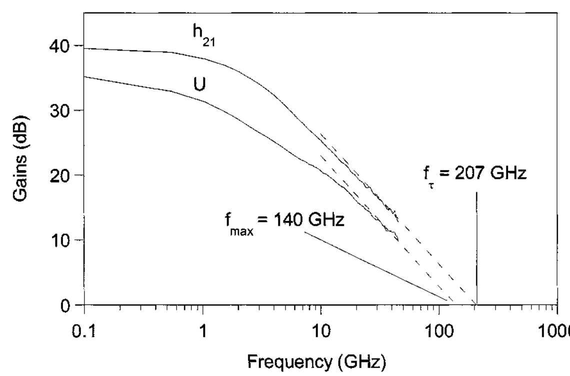

Fig. 3. Measured short-circuit current gain h_{21} and Mason's unilateral power gain U versus frequency for an HBT with a 0.4 μm × 7.5 μm emitter–base junction and a 1.2 μm × 11 μm base–collector junction. $I_C = 12.0$ mA and $V_{CE} = 1.5$ V.

Fig. 2 shows the HBT Gummel [$\log(I_C, I_B)$ versus V_{CE}] characteristics, indicating a collector current ideality factor of 1.1 and a base current ideality factor of 2.2. The characteristics are measured with nonzero (0.3 V) reverse bias applied to the collector–base junction, so that base–collector junction leakage, if present, will be observed. For comparison, Fig. 2 also shows the Gummel characteristics of a large-area HBT (60 μm × 60 μm emitter–base and 100 μm × 130 μm base–collector junctions) fabricated from the same epitaxial material. Despite the large collector–base junction area, the Gummel characteristics indicate that I_{cbo} of the large-area HBT is below 0.1 μA, indicating a collector–base leakage current per unit junction area below 10^{-3} A/cm^2. The small-area HBTs are fabricated on a mask set designed for microwave on-wafer probing calibrated using the line–reflect–line method, and have long (230 μm) 50 Ω coplanar waveguide (CPW) transmission lines between the probe pads and the transistor terminals. The leakage currents observed at low V_{be} in Fig. 2 for the small-area HBT are dominated by leakage currents associated with conduction through the buffer layer between these long interconnects. HBTs are minority-carrier devices, and defect-induced leakage currents resulting from metamorphic growth are potential concerns. Nevertheless, high dc current gains and low $<10^{-3}$ A/cm^2 base–collector leakage are observed.

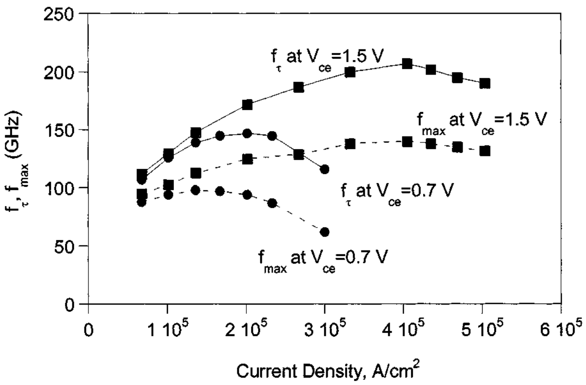

Fig. 4. Measured current-gain cutoff frequency f_τ and power-gain cutoff frequency $f_{\max}$ versus current density at $V_{CE} = 0.7$ V and $V_{CE} = 1.5$ V.

Fig. 3 shows the current gain (h_{21}) and unilateral power gain (U) of the small-area HBT, computed from the measured 0.045–45 GHz S-parameters. A 207 GHz f_τ and a 140 GHz $f_{\max}$ were measured at $I_C = 12.0$ mA (4×10^5 A/cm^2) and $V_{CE} = 1.5$ V, as determined by a -20 dB/decade extrapolation. These are the highest values reported for metamorphic HBTs. Fig. 4 shows the variation of f_τ with collector current density, as measured at $V_{CE} = 0.7$ V and $V_{CE} = 1.5$ V. The observed decrease in f_τ at very high current densities (2.5×10^5 A/cm^2 at $V_{CE} = 0.7$ V, 4.5×10^5 A/cm^2 at $V_{CE} = 1.5$ V) is due to the Kirk effect. HBT junction temperature and thermal resistance were measured by the method of [7]. The 0.4 μm $\times$ 7.5 μm emitter HBTs have a 2.8 K/mW thermal resistance and exhibit a small measured 35 K junction-ambient temperature rise when biased at $J_e = 190$ kA/cm^2 and $V_{ce} = 2$ V ($P/A_E = 380$ kW/cm^2).

REFERENCES

[1] P. Asbeck, F. Chang, K.-C. Wang, G. Sullivan, and D. Cheung, “GaAs-based heterojunction bipolar transistors for very high performance electronic circuits,” *Proc. Inst. Elect. Eng.*, vol. 81, no. 12, pp. 1709–1726, 1993.

[2] Y. Matsuoka, S. Yamahata, K. Kurishima, and H. Ito, “Ultrahigh-speed InP/InGaAs double-heterostructure bipolar transistors and analysis of their operation,” *Jpn. J. Appl. Phys.*, vol. 35, pp. 5646–5654, 1996.

[3] M. W. Dvorak, C. R. Bolognesi, O. J. Pitts, and S. P. Watkins, “300 GHz InP/GaAsSb/InP double HBTs with high current capability and BVCEO $>$ 6V,” *IEEE Electron Device Lett.*, vol. 22, pp. 361–363, Aug. 2001.

[4] H. Q. Zheng, K. Radhakrishnan, H. Wang, K. H. Yuan, S. F. Yoon, and G. I. Ng, “Metamorphic InP/InGaAs double-heterojunction bipolar transistors on GaAs grown by molecular-beam epitaxy,” *Appl. Phys. Lett.*, vol. 77, no. 6, pp. 869–871, 2000.

[5] ——, “Metamorphic InP/InGaAs double-heterojunction bipolar transistors on GaAs grown by molecular-beam epitaxy,” *Appl. Phys. Lett.*, vol. 77, no. 6, pp. 869–871, 2000.

[6] M. J. W. Rodwell, M. Urteaga, Y. Betser, D. Scott, M. Dahlstrom, S. Lee, S. Krishnan, T. Mathew, S. Jaganathan, Y. Wei, D. Mensa, J. Guthrie, R. Pullela, Q. Lee, B. Agarwal, U. Bhattacharya, and S. Long, “Scaling of InGaAs/InAIA’s HBT’s for high speed mixed-signal and mm-wave ICs,” *Int. J. High Speed Electron. Syst.*, vol. 11, no. 1, pp. 159–215, 2001.

[7] W. Liu, H.-F. Chau, and E. Beam, III, “Thermal properties and thermal instabilities of InP-based heterojunction bipolar transistors,” in *IEEE Trans. Electron Devices*: IEEE, Mar. 1996, vol. 43, pp. 388–395.

[8] H.-F. Chau, W. Liu, and E. A. Beam, III, “InP-based HBT’s and their perspective for microwave applications,” in *Proc. 7th Int. Conf. Indium Phosphide and Related Materials*, Hokkaido, Japan, May 9–13, 1995.

[9] M. Sokolich, D. P. Docter, Y. K. Brown, A. R. Kramer, J. F. Jensen, W. E. Stanchina, S. Thomas, III, C. H. Fields, D. A. Ahmari, M. Lui, R. Martinez, and J. A. Duvall, “A low power 52.9 GHz static divider implemented in a manufacturable 180 GHz AlInAs/InGaAs HBT IC technology,” in *Proc. IEEE Gallium Arsenide Integrated Circuit Symp.*, Atlanta, GA, Nov. 1–4, 1998.